



This is a repository copy of *Effects of rapid thermal annealing on telecom C-band InAs quantum dots on InP (100) grown by droplet epitaxy.*

White Rose Research Online URL for this paper:

<https://eprints.whiterose.ac.uk/218658/>

Version: Published Version

Article:

Chan, C.L. orcid.org/0009-0006-8515-3592, Sala, E.M. orcid.org/0000-0001-8116-8830, Clarke, E.M. orcid.org/0000-0002-8287-0282 et al. (1 more author) (2025) Effects of rapid thermal annealing on telecom C-band InAs quantum dots on InP (100) grown by droplet epitaxy. *Journal of Physics D: Applied Physics*, 58 (2). 025107. ISSN 0022-3727

<https://doi.org/10.1088/1361-6463/ad835d>

Reuse

This article is distributed under the terms of the Creative Commons Attribution (CC BY) licence. This licence allows you to distribute, remix, tweak, and build upon the work, even commercially, as long as you credit the authors for the original work. More information and the full terms of the licence here:

<https://creativecommons.org/licenses/>

Takedown

If you consider content in White Rose Research Online to be in breach of UK law, please notify us by emailing eprints@whiterose.ac.uk including the URL of the record and the reason for the withdrawal request.



eprints@whiterose.ac.uk
<https://eprints.whiterose.ac.uk/>

PAPER • OPEN ACCESS

Effects of rapid thermal annealing on telecom C-band InAs quantum dots on InP (100) grown by droplet epitaxy

To cite this article: Chak Lam Chan *et al* 2025 *J. Phys. D: Appl. Phys.* **58** 025107

View the [article online](#) for updates and enhancements.

You may also like

- [VOCs conversion in He/H₂O plasma produced in a micro-capillary tube at atmospheric pressure](#)
G Bauville, M Heninger, J Lemaire *et al.*
- [Investigation of non-equilibrium phenomena in nitrogen RF inductively coupled plasma discharges: a state-to-state approach](#)
Sanjeev Kumar, Alessandro Munafò, Sung Min Jo *et al.*
- [Solution-processed lead halide perovskite films for application in perovskite solar cells: from coating methods to growth dynamics](#)
Yuhuan Xiao and Conghua Zhou



ECS The Electrochemical Society
Advancing solid state & electrochemical science & technology

247th ECS Meeting
Montréal, Canada
May 18-22, 2025
Palais des Congrès de Montréal

Abstracts due December 6th

Showcase your science!

ECS UNITED

Effects of rapid thermal annealing on telecom C-band InAs quantum dots on InP (100) grown by droplet epitaxy

Chak Lam Chan^{1,*} , Elisa Maddalena Sala^{1,2} , Edmund Clarke^{1,2}  and Jon Heffernan^{1,2}

¹ Department of Electronic and Electrical Engineering, The University of Sheffield, North Campus, Broad Lane, Sheffield S3 7HQ, United Kingdom

² EPSRC National Epitaxy Facility, Department of Electronic and Electrical Engineering, The University of Sheffield, North Campus, Broad Lane, Sheffield S3 7HQ, United Kingdom

E-mail: chaklamchan123@hotmail.com

Received 18 April 2024, revised 20 September 2024

Accepted for publication 4 October 2024

Published 17 October 2024



Abstract

We demonstrate the effects of rapid thermal annealing on emission from telecom C-band InAs/InP (100) quantum dots (QDs) grown by droplet epitaxy in metal–organic vapour phase epitaxy. Room temperature photoluminescence from the QD ensemble shows a tuned emission wavelength through the C-band and O-band while improving the emission intensity by ~ 4.5 times at an annealing temperature of 770 °C. A blueshift of the QD emission up to 430 nm has been achieved. Low-temperature micro-photoluminescence demonstrates single QD emission from the annealed samples with an improvement in linewidth of up to 30%.

Keywords: rapid thermal annealing, quantum dots, InAs/InP, droplet epitaxy, MOVPE, photoluminescence

1. Introduction

III–V quantum dots (QDs) play an important role in the active region of various devices for quantum technology applications, such as single photon emitters [1], entangled photon generation [2] and quantum relays [3]. Epitaxial QDs are usually fabricated by Stranski–Krastanov (SK) growth mode [4, 5], but there may be limitations imposed on the growth conditions due to the lattice mismatch between substrate and epilayer [6, 7]. Droplet epitaxy (DE) is an alternative growth method which is more versatile compared to SK and allows for more flexibility in material choice and nanostructure fabrication [8]. Most importantly, highly symmetric QDs can be obtained using DE, showing reduced fine structure splitting (FSS) and longer coherence times [6, 7, 9]. Thus, QDs grown

by the DE method are promising candidates as high-quality single-photon emitters [8, 10–12].

Altering the structure of the QDs using post-growth techniques can be used to obtain QDs with more favourable optical properties for photonics applications. For example as-grown QDs may show a spectral distribution longer than the targeted wavelengths—in our case, the important telecoms C-band and O-band. The use of post-growth methods, such as ion implantation [13], electric fields [13], and optical stark effect [14], have all been shown to control the QDs emission brightness [12], wavelength [15], and FSS [16]. Rapid thermal annealing (RTA) is a well-known technique that has been shown to improve the structural and optical properties of self-assembled QDs [15, 17, 18]. For instance, thermal treatments have been shown to remove defects and allow interdiffusion mechanisms to take place, resulting in shifted emission wavelengths [19], brightness enhancement [15] and reduction in the inhomogeneously-broadened linewidth of emission from the QD ensemble [20].

In this study, we investigate the effects of RTA on the optical properties of C-band emitting InAs/InP (100) QDs grown by DE in metal–organic vapour phase epitaxy

* Author to whom any correspondence should be addressed.



Original content from this work may be used under the terms of the [Creative Commons Attribution 4.0 licence](https://creativecommons.org/licenses/by/4.0/). Any further distribution of this work must maintain attribution to the author(s) and the title of the work, journal citation and DOI.

(MOVPE). When annealed up to 800 °C, a large room temperature photoluminescence (RT-PL) blueshift of 430 nm is observed, and the associated ensemble linewidth narrows by 15% (~ 50 meV). We also report on single-dot spectroscopy measured using low-temperature (5 K) micro-photoluminescence (LT- μ PL), where a blueshift of single QD emission toward 1300 nm is observed, and single-dot linewidths showed an improvement by up to 30% (~ 20 μ eV).

2. Methods

Samples were grown on epi-ready InP(001) in a closed-coupled showerhead MOVPE reactor, using H₂ as carrier gas. No pre-treatment was used on the samples prior to growth. Indium droplets were deposited on a 300 nm InP buffer grown at 620 °C. Droplets were deposited at 320 °C and then crystallised into InAs QDs under an AsH₃ flow while ramping the temperature to 520 °C. The conditions used for QD growth were previously optimised to achieve high-quality InAs QDs showing LT single-dot emission at wavelengths around 1550 nm [21, 22]. After droplet crystallisation into InAs QDs, an InP capping layer of 20 nm was deposited at the same crystallisation temperature of 520 °C. A further 80 nm InP was grown at 620 °C to bury the QDs entirely. We refer to our previous works for additional information on the growth sequence [21, 22]. Such QDs are grown from metallic droplets, however they will be strained after complete crystallisation and burying process with InP, or be partially relaxed, akin to what happens to SK dots. A set of 5 × 5 mm² samples was annealed with the use of proximity capping between 650 °C and 850 °C (including an unannealed as-grown sample for reference), where sacrificial InP substrate was used to prevent the outdiffusion of group V atoms [15]. Another set of samples was capped with 100 nm SiO₂ (40 nm/min) by plasma-enhanced chemical vapour deposition to protect the surface during RTA. After dielectric capping, the samples were cleaved into 5 × 5 mm² pieces before being annealed at temperatures ranging from 750 °C to 800 °C for 30 s including another reference sample (as-grown) which was SiO₂ capped but not annealed. For both set of experiments, samples were taken from locations on the wafer in close proximity to each other, to ensure the annealing effects would be comparable. The samples were cleaved into 5 × 5 mm² pieces before being annealed at temperatures ranging from 750 °C to 800 °C for 30 s. The samples were placed into two different PL setups for RT-PL and LT- μ PL. For RT-PL, the samples were measured using an Accent RPM2000 PL mapper, with excitation from a 656 nm diode laser with the PL dispersed by a 150 g mm⁻¹ grating and detected with a Hamamatsu G9208 InGaAs detector with an extended response up to 2200 nm. Next, the same QD samples were investigated by LT- μ PL at 5 K. For μ PL, the samples were excited via a fibre-coupled 635 nm red diode laser at approximately 4.5 W cm⁻² with a Princeton Instruments SP2750 spectrometer and 600 lines/mm grating and a cooled PyLoN IR InGaAs detector. The response

of the InGaAs detector on the LT- μ PL system is limited to 1600 nm, so single QD emission at longer wavelengths may not be detected.

3. Results and discussions

3.1. RT-PL

Figure 1 shows the RT-PL spectra obtained from samples annealed at different temperatures with either proximity capping or SiO₂ capping. With proximity capping, we do not observe a blueshift of ensemble emission or significant changes in PL intensity up to an annealing temperature of 850 °C as a result of lack of interdiffusion between InAs QD and adjacent InP layers. While the ensemble does not shift under annealing, minor changes to the individual peaks of the ensemble are still observed, suggesting a gradual degradation of the sample or outdiffusion of indium atoms, which could impact the carrier dynamics. With the use of SiO₂ capping, the PL intensity doubles starting at 750 °C to a maximum increase in PL intensity of ~ 4.5 times at 770 °C when compared to as-grown. Subsequent annealing temperatures give no further improvement in PL intensity. This is consistent with previous reports of an increase of ~ 3 times in PL intensity from InAs/InP QDs with annealing when compared to an as-grown sample [23]. The PL intensity increase can be attributed to an annealing-induced reduction in defects and other non-radiative recombination centres [24–26]. Increasing the annealing temperature above 770 °C results in the degradation of the material quality, causing the generation of unwanted dislocations and outdiffusion of indium atoms [17, 23, 27]. We also observe a general narrowing of the ensemble PL FWHM with increasing annealing temperature, as shown in figure 2, with the lowest FWHM of 329 meV (770 °C), compared to 378 meV (as-grown). The FWHM of the as-grown ensemble is large but comparable with that observed by other groups for InAs/InP QDs emitting at these wavelengths [28, 29]. Modified growth conditions that blueshift the QD emission towards 1550 nm, such as indium-flush or growth on InGaAs interlayers [29, 30], yield QD ensembles with narrower FWHM but we would still expect annealing to result in a further reduction in FWHM for QDs grown using these techniques. For RTA, the narrowing of FWHM is linked to the changing of the QD shape and compositions, as demonstrated by other groups [23, 31, 32]. This is made possible with the use of SiO₂ layers, which have previously been demonstrated to allow for promotion to impurity-free vacancy disordering, an additional mechanism assisting indium and group-V outdiffusion. This results in the blueshift of emission from compositional changes in the QDs due to intermixing as well as narrowing of the ensemble linewidth due to the increase in QD size and uniformity of the QD ensemble [32]. We also observe the formation of microcracks during high-temperature annealing [23]. The disappearance of individual peaks across the ensemble could also be attributed to the degradation of the sample and linked to the outdiffusion of indium atoms from the structure into the SiO₂ layer.

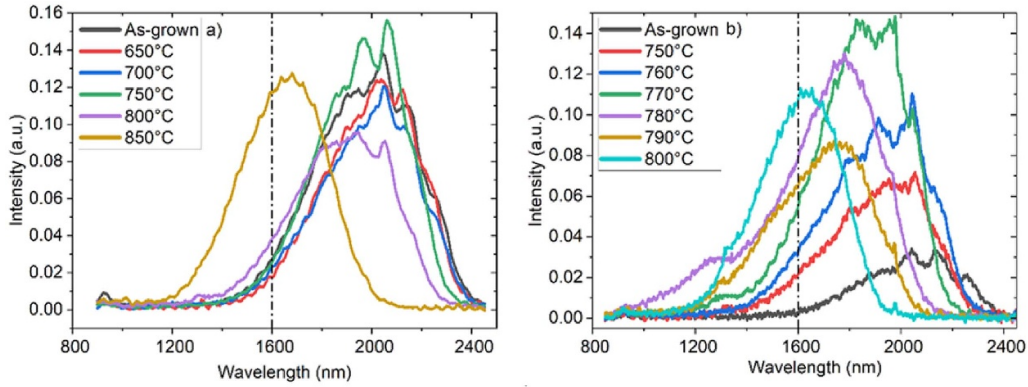


Figure 1. Room temperature PL for (a) proximity cap between annealing temperature 650 °C–850 °C compared with as-grown, (b) SiO₂ cap with annealing temperature 750 °C–800 °C compared with as-grown. Dot-dash line indicating the μ PL detector’s cut-off.

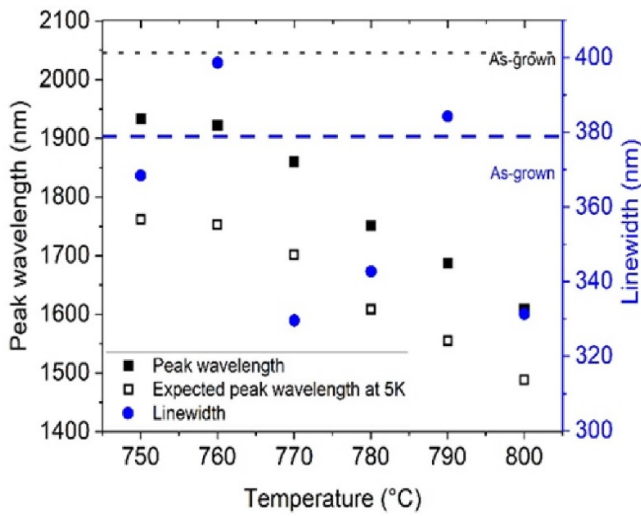


Figure 2. Gaussian fitted analysis of annealing temperature against peak wavelength (solid squares) and linewidth (circles), with the dashed lines showing as-grown comparisons for SiO₂ capped sample. The expected peak wavelength of the ensemble at 5 K, according to the Varshni relation, is also included (open squares) [36].

The peak wavelength emissions can be controlled by varying the annealing temperature, as summarised in figure 2. Comparing the different capping methods used, we observed a change in annealing temperature by 50 °C before blueshifting occurred. One known cause is the significant difference in thermal expansion coefficients between SiO₂ ($\sim 0.52 \times 10^{-6} \text{ }^\circ\text{C}^{-1}$) and InP ($\sim 4.6 \times 10^{-6} \text{ }^\circ\text{C}^{-1}$). This causes compressive stress at the interface region during annealing, which will allow for group-V intermixing more readily [33]. This mechanism is in contrast with InAs/GaAs QDs structures where such interaction is between In/Ga atoms instead [19, 34, 35]. The effect of indium and group-V out-diffusion is also a common mechanism alongside intermixing of As/P atoms across the interfaces of InAs QDs and InP barriers [31, 32]. This results in the largest blueshift of 430 nm,

which is observed with an annealing temperature of 800 °C with SiO₂ capping. The improvement in optical properties is attributed to the change in the capping method, which allows vacancies to form when outdiffusion of indium and group-V atoms [23] while also protecting the surface from excessive surface degradation [17]. Repeating the same annealing experiment on different regions of the same wafer, produces comparable PL results. As such, we ascribe such effects to the use of different capping methods. With promising results from RT-PL, the single dot spectrum of the SiO₂ capped sample was measured using LT- μ PL to understand the effects RTA has on single dot emissions.

3.2. LT- μ PL

The RT-PL measurements presented in figure 1 allow us to identify the wavelength range of the whole ensemble. Still, when considering the portion of the ensemble visible by LT- μ PL (5 K), this is limited by the detection range (1300 nm–1600 nm). We expect an average emission blueshift of ~ 150 nm for the QD ensemble between RT and 5 K following the Varshni relation, shown in figure 2 [37]. Annealing the samples blueshifts the ensemble emission towards the detection range of the LT- μ PL so the spectra obtained from the as-grown sample are from QDs at the short-wavelength edge of the ensemble. The sample annealed at 780 °C would best represent the peak ensemble range of QDs, which has improved linewidth distribution when compared to the as-grown sample, the short-wavelength edge. Similarly, at higher annealing temperatures, emissions originating from the long-wavelength edge of the QD distribution have comparable linewidths to the peak of the ensemble for the as-grown sample.

Figure 3 shows examples of μ PL spectra of SiO₂ capped samples annealed at (a) 800 °C, (b) 770 °C, (c) 750 °C and (d) as-grown. In the as-grown sample, a high density of sharp emissions from single QDs is seen alongside background noise. The background noise observed is possibly caused by significant charge noise, leading to emission broadening and

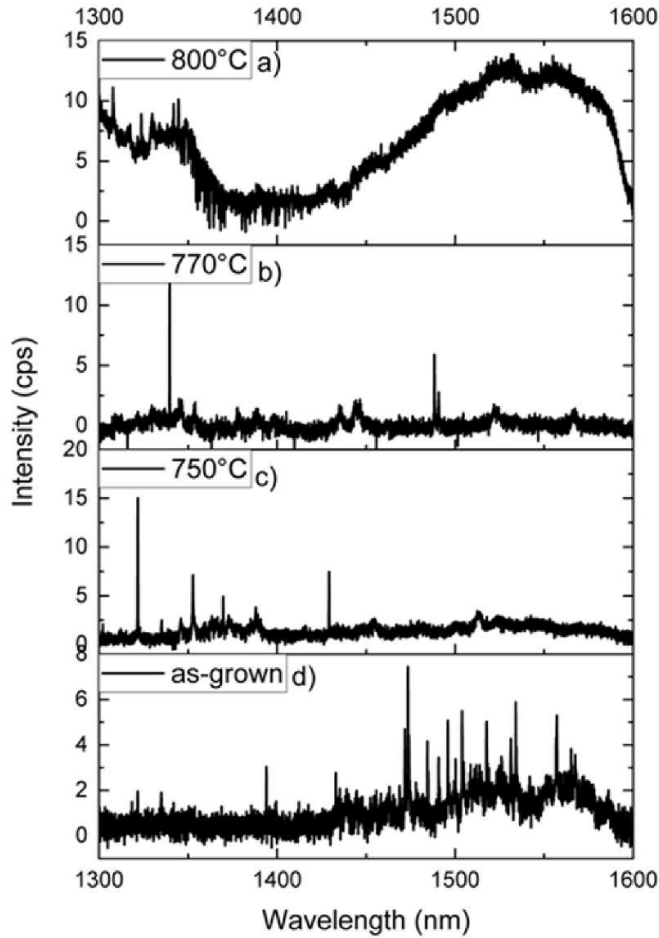


Figure 3. μ pl single dot spectra of SiO_2 capped samples at 5 K for (a) 800 °C, (b) 770 °C, (c) 750 °C, (d) as-grown.

coalescence of emission peaks [38]. At 750 °C, the background noise is quenched, most likely due to a reduction of defects after annealing. Blueshifting of sharp dot-like emissions is observed after annealing, emitting around 1300 nm. The density of dot-like emissions has decreased, but there is no evidence of emission broadening. At 770 °C, we observe the most significant improvement in linewidth while maintaining dot-like sharp emissions and a significant reduction in background noise. At 800 °C, background noise reappears, which extends across the entire range with the atmosphere absorption range from 1350 nm to 1450 nm. We believe factors such as microcrack formation cause the observed increase in background noise at high annealing temperatures. This is also consistent with the observed reduction in integrated PL intensity shown in figure 1 [23]. Between 750 °C–770 °C, bright, narrow emission lines from single QDs can be detected in the range 1300–1500 nm. To statistically analyse the distribution of single dot-like emissions, multiple single spectra were obtained at each annealing temperature [37].

Figures 4(a)–(g) shows a comparison of sharp dot-like emissions between annealed and as-grown QDs. As-grown single spectra show good emission between 1400 nm to 1550 nm, with comparable results when multiple locations

across the sample are measured. With increasing annealing temperature, we observe additional dot-like emission between 1400 nm and our short-wavelength measurement limit of 1300 nm. By comparison, with the RT ensemble PL shown in figure 1 and the expected peak ensemble wavelength at the low temperature shown in figure 2, the QD distribution shown in figure 4 matches the expected wavelengths according to Varshni's relation. For the annealed samples, the blueshift will shift the short-wavelength side of the ensemble below 1300 nm at low temperature, allowing observation of single QD emission between 1300–1400 nm in our μ -PL measurements. With increasing annealing temperature, we may obtain a blueshift of the emission beyond the short-wavelength limit of our measurements at 1300 nm from an increased number of QDs in the distribution due to the outdiffusion of indium from the QDs. It is surprising that we do not observe single QD emission >1500 nm for the samples annealed at 750 and 760 °C. This may be due to statistical variations in the spectra, as we observe QD emission >1500 nm for samples annealed at higher temperatures, and the RT PL suggests that the QDs observed in μ PL are on the short-wavelength side of the QD distribution for all samples. QD emission around 1400 nm may be suppressed by atmospheric absorption, with fewer emission lines from the QDs being above the noise floor of the detector and resulting in an apparent bimodal wavelength distribution in the data presented in figure 4. The sudden formation of bimodal distribution on a single-dot level is currently still unknown. This could be linked to the disappearance of individual peaks observed in figure 1, where the high temperature used may have caused outdiffusion of indium atoms from the QDs, affecting the QD morphology and thus the carrier dynamics [39].

To understand how RTA affected single QD properties and its relationship between emission shifting and linewidth, we define two groups of emission lines in the spectra from the annealed samples: group 1 is defined as dot emissions below 1425 nm corresponding to QDs whose emission has been blueshifted to wavelengths shorter than the emission from the as-grown sample, while group 2 is emissions above 1425 nm, corresponding to QDs whose emission will also have been blueshifted due to annealing but are emitting at wavelengths comparable to the as-grown sample. Figures 4(h)–(n) shows the linewidth distribution for single QD emission as a function of different annealing temperatures. Below 770 °C, the linewidths are comparable to those obtained from the as-grown sample. For annealing temperature of 770 °C and above, we observe an improvement in the linewidth distributions, with the lowest linewidth of 22.0 μeV (790 °C), close to the detector spectral resolution of 20.9 μeV . An increase in the number of emission lines with large linewidth for the sample annealed at 800 °C is consistent with material degradation, that may also contribute to the increased background emission observed for this sample. We do not observe a significant difference in the linewidths of emission lines from QDs in groups 1 and 2, where low linewidth QDs are maintained across the wavelength range. This demonstrates that the improvement to linewidth is not dependent on emission wavelength and

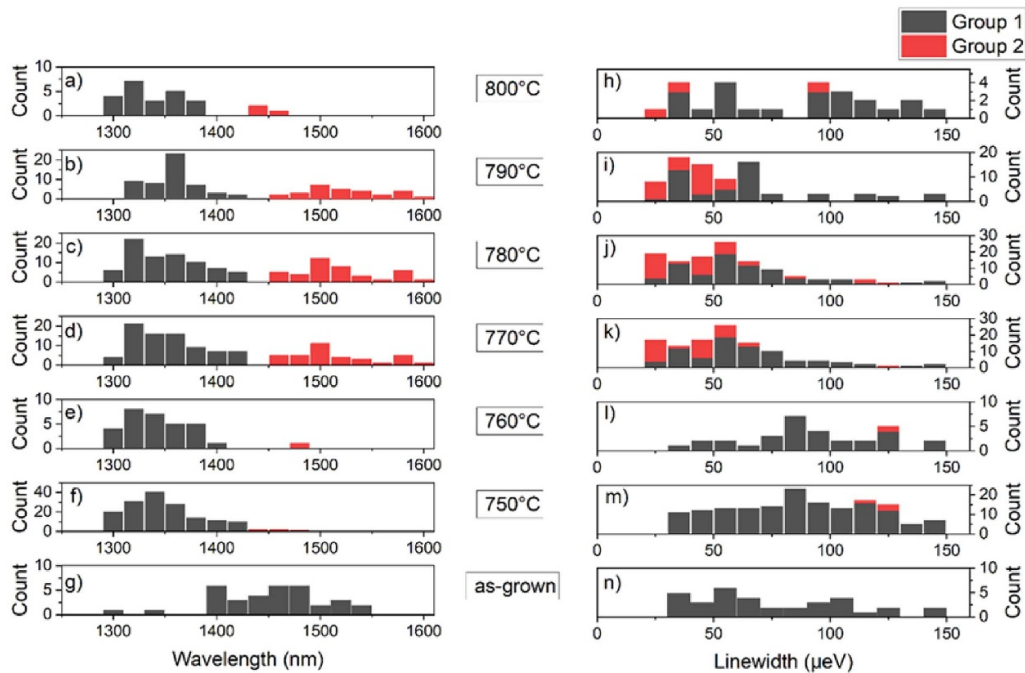


Figure 4. Histogram analysis of multiple single dot emissions of SiO₂ capped sample at 5 K for wavelength distribution of (a) 800 °C, (b) 790 °C, (c) 780 °C, (d) 770 °C, (e) 760 °C, (f) 750 °C, (g) as-grown, and linewidth distribution of (h) 800 °C, (i) 790 °C, (j) 780 °C, (k) 770 °C, (l) 760 °C, (m) 750 °C, (n) as-grown. Single dot emissions are further split QD emissions below 1425 nm (black/group1), above 1425 nm (red/group2).

demonstrates that the use of RTA can be beneficial for improving the QD linewidth for samples targeting either the O-band or the C-band.

4. Conclusion

In conclusion, we have examined the impact of RTA on telecom InAs QDs on InP grown by DE in MOVPE. By varying the annealing temperature above 750 °C, a controllable blueshift of the QD ensemble emission up to 430 nm under RT-PL conditions is observed. RTA also increases the integrated intensity and decreases the PL linewidth. In μ PL, the emission of the QDs can be blueshifted to the O-band. At annealing temperatures of 770 °C and above, we achieved an improvement of 30% (~ 20 μ eV) in single QD emission linewidth. Control of the annealing temperature gives the ability to adjust the emission wavelength and reduce the emission linewidth from single dots, enhancing the potential of InAs/InP DE QDs embedded in quantum devices.

Data availability statement

All data that support the findings of this study are included within the article (and any supplementary files).

Acknowledgment

We wish to acknowledge the support by EPSRC Grant EP/R03480X/1, and the InnovateUK project QFoundry.

ORCID iDs

Chak Lam Chan  <https://orcid.org/0009-0006-8515-3592>

Elisa Maddalena Sala  <https://orcid.org/0000-0001-8116-8830>

Edmund Clarke  <https://orcid.org/0000-0002-8287-0282>

References

- [1] Michler P, Kiraz A, Becher C, Schoenfeld W V, Petroff P M, Zhang L, Hu E and Imamoğlu A 2000 *Science* **290** 2282–5
- [2] Stevenson R M, Young R J, Atkinson P, Cooper K, Ritchie D A and Shields A J 2006 *Nature* **439** 179–82
- [3] Huwer J, Stevenson R M, Skiba-Szymanska J, Ward M B, Shields A J, Felle M, Farrer I, Ritchie D A and Pentry R V 2017 *Phys. Rev. Appl.* **8** 024007
- [4] Goldstein L, Glas F, Marzin J Y, Charasse M N and Le Roux G 1985 *Appl. Phys. Lett.* **47** 1099–101
- [5] Eaglesham D J and Cerullo M 1990 *Phys. Rev. Lett.* **64** 1943
- [6] Anderson M, Müller T, Skiba-Szymanska J, Krysa A B, Huwer J, Stevenson R M, Heffernan J, Ritchie D A and Shields A J 2020 *Appl. Phys. Lett.* **118** 1
- [7] Skiba-Szymanska J *et al* 2017 *Phys. Rev. Appl.* **8** 014013
- [8] Gurioli M, Wang Z, Rastelli A, Kuroda T and Sanguinetti S 2019 *Nat. Mater.* **18** 799–810
- [9] Müller T, Skiba-Szymanska J, Krysa A B, Huwer J, Felle M, Anderson M, Stevenson R M, Heffernan J, Ritchie D A and Shields A J 2018 *Nat. Commun.* **9** 12
- [10] Gajjala R S R, Sala E M, Heffernan J and Koenraad P M 2022 *ACS Appl. Nano Mater.* **5** 8070–9
- [11] Sala E M, Na Y I, Godsland M and Heffernan J 2024 *Phys. Status Solidi* **18** 2300340
- [12] Phillips C L *et al* 2024 *Sci. Rep.* **14**–1 1–9
- [13] Dion C, Desjardins P, Chicoine M, Schiettekatte F, Poole P J and Raymond S 2007 *Nanotechnology* **18** 015404

- [14] Reimer M E, Korkusiński M, Dalacu D, Lefebvre J, Lapointe J, Poole P J, Aers G C, McKinnon W R, Hawrylak P and Williams R L 2008 *Phys. Rev. B* **78** 11
- [15] Muller A, Fang W, Lawall J and Solomon G S 2009 *Phys. Rev. Lett.* **103** 11
- [16] Babiński A, Jasiński J, Bozek R, Szepielow A and Baranowski J M 2001 *Appl. Phys. Lett.* **79** 2576–8
- [17] Plumbhof J D, Trotta R, Rastelli A and Schmidt O G 2012 *Nanoscale Res. Lett.* **7** 336
- [18] Chaâbani W, Melliti A, Maaref M A, Testelin C and Lemaître A 2016 *Physica B* **493** 53–57
- [19] García J M, Medeiros-Ribeiro G, Schmidt K, Ngo T, Feng J L, Lorke A, Kotthaus J and Petroff P M 1997 *Appl. Phys. Lett.* **71** 2014–6
- [20] Yang T, Tatebayashi J, Aoki K, Nishioka M and Arakawa Y 2007 *Appl. Phys. Lett.* **90** 111912
- [21] Xu S J, Wang X C, Chua S J, Wang C H, Fan W J, Jiang J and Xie X G 1998 *Appl. Phys. Lett.* **72** 3335–7
- [22] Sala E M, Godsland M, Trapalis A and Heffernan J 2021 *Phys. Status Solidi* **15** 2100283
- [23] Sala E M, Na Y I, Godsland M, Trapalis A and Heffernan J 2020 *Phys. Status Solidi* **14** 2000173
- [24] Chia C K, Chua S J, Tripathy S and Dong J R 2005 *Appl. Phys. Lett.* **86** 1–3
- [25] Sakai J W L and Morais P C 2001 *Solid State Commun.* **120** 89–93
- [26] Jiang W H, Xu H Z, Xu B, Ye X L, Wu J, Ding D, Liang J B and Wang Z G 2000 *J. Cryst. Growth* **212** 356–9
- [27] Lee E G, Kim M D and Lee D 2006 *J. Korean Phys. Soc.* **48** 1228–32
- [28] Hasan S, Richard O, Merckling C and Vandervorst W 2021 *J. Cryst. Growth* **557** 126010
- [29] Park K, Moon P, Ahn E, Hong S, Yoon E, Yoon J W, Cheong H and Leburton J-P 2005 *Appl. Phys. Lett.* **86** 223110
- [30] Sala E M, Godsland M, Na Y I, Trapalis A and Heffernan J 2022 *Nanotechnology* **33** 065601
- [31] Malik S, Roberts C, Murray R and Pate M 1997 *Appl. Phys. Lett.* **71** 1987–9
- [32] Dion C, Desjardins P, Shtinkov N, Schiettekatte F, Poole P J and Raymond S 2008 *J. Appl. Phys.* **103** 083526
- [33] Girard J F, Dion C, Desjardins P, Ni Allen C, Poole P J and Raymond S 2004 *Appl. Phys. Lett.* **84** 3382–4
- [34] Barik S, Fu L, Tan H H and Jagadish C 2007 *Appl. Phys. Lett.* **90** 243114
- [35] Kosogov A O *et al* 1996 *Appl. Phys. Lett.* **69** 3072–4
- [36] Varshni Y P 1967 *Physica* **34** 149–54
- [37] Hsu T M, Lan Y S, Chang W H, Yeh N T and Chyi J I 2000 *Appl. Phys. Lett.* **76** 691–3
- [38] Xiaohong T, Zongyou Y, Jinghua T, Anyan D and Mee Koy C 2008 *IEEE Trans. Nanotechnol.* **7** 422–6
- [39] Lei W, Chen Y H, Wang Y L, Xu B, Ye X L, Zeng Y P and Wang Z G 2005 *J. Cryst. Growth* **284** 20–27